



## Knockdown of RhoQ, a member of Rho GTPase, accelerates TGF- $\beta$ -induced EMT in human lung adenocarcinoma

Kotone Satoh<sup>a</sup>, Satoshi Sakai<sup>b</sup>, Makoto Nishizuka<sup>a,\*</sup>

<sup>a</sup> Department of Applied Biology and Food Sciences, Faculty of Agriculture and Life Science, Hirosaki University, 3 Bunkyo-cho, Hirosaki, Aomori, 036-8561, Japan

<sup>b</sup> Department of Molecular Biology, Hamamatsu University School of Medicine, 1-20-1 Handayama, Higashi-ku, Hamamatsu, Shizuoka, 431-3192, Japan

### ARTICLE INFO

#### Keywords:

EMT  
RhoQ  
Lung adenocarcinoma  
TGF- $\beta$

### ABSTRACT

Lung cancer is the leading cause of cancer-related deaths worldwide, and the most common subtype of lung cancer is adenocarcinoma. RhoQ is a Rho family GTPase with primary sequence and structural similarities to Cdc42 and RhoJ. RhoQ is involved in neurite outgrowth via membrane trafficking and is essential for insulin-stimulated glucose uptake in mature adipocytes. However, the function of RhoQ in lung adenocarcinoma (LUAD) remains unclear. In this study, RhoQ siRNAs were introduced into A549 and PC-9 cells. Expression level of EMT-related genes and invasion ability were investigated using Western blot and transwell assay. To examine the relationship between RhoQ expression and prognosis of LUAD, Kaplan–Meier plotter was used. We discovered that suppressing RhoQ expression promoted TGF- $\beta$ -mediated EMT and invasion in LUAD cell lines. Furthermore, RhoQ knockdown increased Smad3 phosphorylation and Snail expression, indicating that RhoQ was involved in TGF/Smad signaling during the EMT process. Moreover, Kaplan–Meier plotter analysis revealed that low RhoQ levels were associated with poor overall survival in patients with LUAD. In conclusion, these findings shed light on RhoQ's role as a negative regulator of TGF- $\beta$ -mediated EMT in LUAD.

### 1. Introduction

Lung cancer has the highest morbidity and mortality rates of any cancer type, accounting for 1.8 million cancer-related deaths globally in 2020 [1]. Non-small cell lung cancer (NSCLC) is the primary component of lung cancer, with lung adenocarcinoma (LUAD) being the most frequently diagnosed histological subtype [2]. With an overall survival rate of fewer than 5 years, LUAD is one of the most invasive and rapidly fatal tumor types. As a result, further research into the molecular mechanism of LUAD metastasis is critical for developing effective therapies.

The occurrence of epithelial-to-mesenchymal transition (EMT) promotes invasiveness and metastasis in lung cancer progression [3]. During the EMT process, epithelial cells lose their polarity and become invasive, transforming into mesenchymal stem cells with migratory and invasive abilities [4]. Extracellular stimuli from the tumor microenvironment, such as growth factors, inflammatory cytokines, and physical

stresses such as hypoxia, regulate EMT [5]. Furthermore, it is well known that many transcription factors, including snail and slug, are involved in EMT regulation [6]. These findings suggest that EMT is governed by a complex mechanism influenced by various factors. The molecular mechanism regulating EMT must be understood to identify new therapeutic targets for LUAD.

We recently found that inhibiting RhoJ expression, a protein in the Rho family of small GTPases, promoted TGF- $\beta$ -induced EMT in LUAD A549 cells [7]. Furthermore, Zeng et al. discovered that RhoJ expression was lower in patients with LUAD than in healthy people and higher RhoJ expression was associated with longer survival times in patients with NSCLC [8]. According to these findings, decreased RhoJ expression may increase NSCLC metastatic potential and poor prognosis by promoting EMT. RhoJ is 85% similar to RhoQ and 78% similar to the cell division cycle (cdc42) with respect to amino acid sequence [9]. Cdc42 is an essential member of the Rho family, and it regulates the cell cycle, controls gene transcription, and regulates the cytoskeleton, cell

**Abbreviations:** Cdc42, Cell division cycle 42; DMEM, Dulbecco's Modified Eagle's Medium; EMT, Epithelial-to-Mesenchymal Transition; FBS, Fetal Bovine Serum; ERK, Extracellular signal-related kinase; LUAD, Lung adenocarcinoma; MEK, Mitogen-activated protein kinase kinase; NSCLC, Non-Small-Cell Lung Cancer; qPCR, Quantitative Polymerase Chain Reaction; rRNA, Ribosomal ribonucleic acid; SDS, Sodium Dodecyl Sulfate; siRNA, Small Interfering RNA; TGF- $\beta$ , Transforming Growth Factor-beta; TRITC, tetramethylrhodamine-isothiocyanate.

\* Corresponding author.

E-mail address: [nishizuka@hirosaki-u.ac.jp](mailto:nishizuka@hirosaki-u.ac.jp) (M. Nishizuka).

<https://doi.org/10.1016/j.bbrep.2022.101346>

Received 5 July 2022; Received in revised form 30 August 2022; Accepted 8 September 2022

2405-5808/© 2022 The Authors. Published by Elsevier B.V. This is an open access article under the CC BY-NC-ND license (<http://creativecommons.org/licenses/by-nc-nd/4.0/>).

movement, and polarization [10]. According to some reports, cdc42 was involved in the EMT process of lung cancer. In human lung cancer, for example, the release of p120-catenin from the adherence junctions to the cytoplasm, which leads to E-cadherin degradation, has been associated with cdc42 activation [11]. Dong et al. demonstrated that miR-186 decreased the invasion of human lung cancer cells by directly targeting cdc42 and modulating EMT [12]. According to these findings, cdc42 may promote EMT in lung cancer.

RhoQ, also known as TC10, was originally cloned from a human teratocarcinoma cDNA library [13]. RhoQ is involved in neurite outgrowth via membrane trafficking and cytoskeleton reorganization [14]. Furthermore, RhoQ interacts with Exo70, a component of the exocyst tethering complex, and plays a vital role in membrane expansion at the growth cones in hippocampal neurons and PC12 cells [15]. Furthermore, RhoQ has been shown to be important in insulin-stimulated glucose uptake and the translocation of the glucose transporter GLUT4 in adipocytes [16]. Although RhoQ has not been proven to be a key player in cancer metastasis, several studies have shown that RhoQ is involved in cancer metastasis. RhoQ is found at invadopodia, actin-rich plasma membrane protrusions, and helps to regulate exocytic vesicular at invadopodia, which is involved in matrix degradation, invasion, and metastasis of breast cancer [17]. Furthermore, Han et al. reported that colorectal cancer cells frequently exhibit a novel A-to-I editing of RhoQ transcripts, resulting in amino acid substitution that promotes invasion [18]. However, the role of RhoQ in lung cancer is unknown.

In the current study, we investigated the role of RhoQ in TGF- $\beta$ -mediated EMT in LUAD cell lines. We discovered that knockdown of RhoQ accelerated EMT by regulating TGF- $\beta$ /Smad signaling and promoted LUAD invasion capacity. Furthermore, patients with LUAD with lower RhoQ expression had a lower survival rate than those with higher RhoQ expression. Our findings suggest that RhoQ is a key regulator of TGF- $\beta$ -mediated EMT and invasion in LUAD.

## 2. Materials and methods

### 2.1. Cell culture

The human LUAD cell lines A549 and PC-9 were obtained from RIKEN Cell Bank. A549 cells were grown in high-glucose Dulbecco's modified Eagle's medium (DMEM) with 10% fetal bovine serum (FBS). PC-9 cells were cultured in RPMI1640 supplemented with 10% FBS. A549 and PC-9 cells were treated with recombinant human TGF- $\beta$ 1 at 1 or 5 ng/mL concentrations obtained from R&D systems, respectively [19,20].

### 2.2. RNA interference experiments

Two different human RhoQ siRNAs (siRhoQ-A and siRhoQ-B) were designed and synthesized at NIPPON GENE. The sequences of siRhoQ-A and siRhoQ-B were 5'-UGACCGAUGUCUCCUUA-3' and 5'-GGAUCAAGAUGUAUAAACU-3', respectively. Luciferase siRNA, 5'-CGUACGCGGAAUACUUCGATT-3', was also obtained from NIPPON GENE and used as a control. siRNAs transfection was performed using Lipofectamine2000 according to the manufacturer's instructions.

### 2.3. F-actin staining

The cells were washed three times with ice-cold PBS and fixed for 10 min in 2% paraformaldehyde. The cells were stained with tetramethylrhodamine isothiocyanate (TRITC)-conjugated phalloidin to detect the F-actin structure [21].

### 2.4. Quantification of elongated cell morphology

Elongated cell morphology was evaluated as previously described

[22]. The lengths of the major and minor cell axes were measured using NIH-Image software, and cell ratios of major to minor axes were used to determine the degree of elongated cell morphology.

### 2.5. Western blotting

Radio-immunoprecipitation assay buffer [150 mM NaCl, 50 mM Tris-HCl (pH 8.0), 1% Nonidet-P40, 1% sodium dodecyl sulfate (SDS), 0.5% deoxycholate] supplemented with a protease inhibitor cocktail and a phosphatase inhibitor cocktail was used to prepare cell lysates. SDS-PAGE was used to separate equal amounts of total protein, which was then transferred to a polyvinylidene difluoride membrane. The membranes were blocked in 3% nonfat dry milk before being immunoblotted with primary antibodies specific for E-cadherin, N-cadherin, Snail, phospho-Smad3, total-Smad3 (1/1000; Cell Signaling Technology), fibronectin (1/500; Santa Cruz Biotechnology), RhoQ (1/2500; abcam), and  $\beta$ -actin (1/8000; SIGMA). After washing, the membranes were incubated with horseradish peroxidase-conjugated secondary antibodies (1/10,000; Jackson ImmunoResearch Laboratories). The membranes were then developed using the ECL Chemiluminescence Kit (Amersham) and bands were detected by exposure to X-ray film. The blots were quantified using NIH-Image software.

### 2.6. Quantitative real-time PCR

Total RNA was extracted using the TRI reagent (SIGMA-Aldrich) as directed by the manufacturer. Subsequently, cDNA was synthesized using a ReverTra Ace (ToYoBo) as per the manufacturer's protocol. The expression levels of mRNA were determined using Brilliant III Ultra-Fast SYBR Green QPCR Master Mix (Agilent). Primers for detection of human RhoQ were purchased from Origene. The primers used in each reaction were as follows: human E-cadherin [23]: forward 5'-CCAGAAACGGAGGCCTGAT-3', reverse 5'-CTGGGACTCCACCTACAGAAAGTT-3'; human fibronectin [24]: forward 5'-GTGTTGGGAATGGTCTGTTGGGAATG-3', reverse 5'-CCAATGCCACGGCCATAGCAGTAGC-3'; and human 18S rRNA [7]: forward 5'-CTCAACACGGGAAACCTCAC-3', reverse 5'-AGACAAATCGCTCCACCAAC-3'.

### 2.7. Invasion assays

The invasion assay was performed using Transwell 24-well plates with 8  $\mu$ m pore polycarbonate membranes as previously described [25]. Matrigel was applied to the upper side of the membranes (Corning). After 1 ng/ml TGF- $\beta$ 1 treatment for 48 h, A549 cells transfected with control or siRhoQ-A were placed in a serum-free medium in the upper chamber. The lower chamber was filled with high-glucose DMEM containing 10% FBS. After 24 h of incubation, cells on the upper surface of the membrane were gently scrubbed away with cotton swabs. The chambers were then fixed in 2% paraformaldehyde for 10 min before stained with crystal violet. Five randomly selected fields in each well were photographed and counted. The relative invasion cell number was calculated from the mean value relative to Luc (-), set as 1.

### 2.8. Cell proliferation assays

After treatment of TGF- $\beta$ 1 for 48 h, RhoQ-knockdown and control cells were seeded into 24-well plates at a density of  $1 \times 10^4$  cells/well. After 24 h, cells were trypsinized and counted.

### 2.9. In silico analysis

The online Kaplan–Meier plotter (<http://kmpplot.com/analysis/>) was used to examine the correlation between RhoQ and human lung cancers [26].

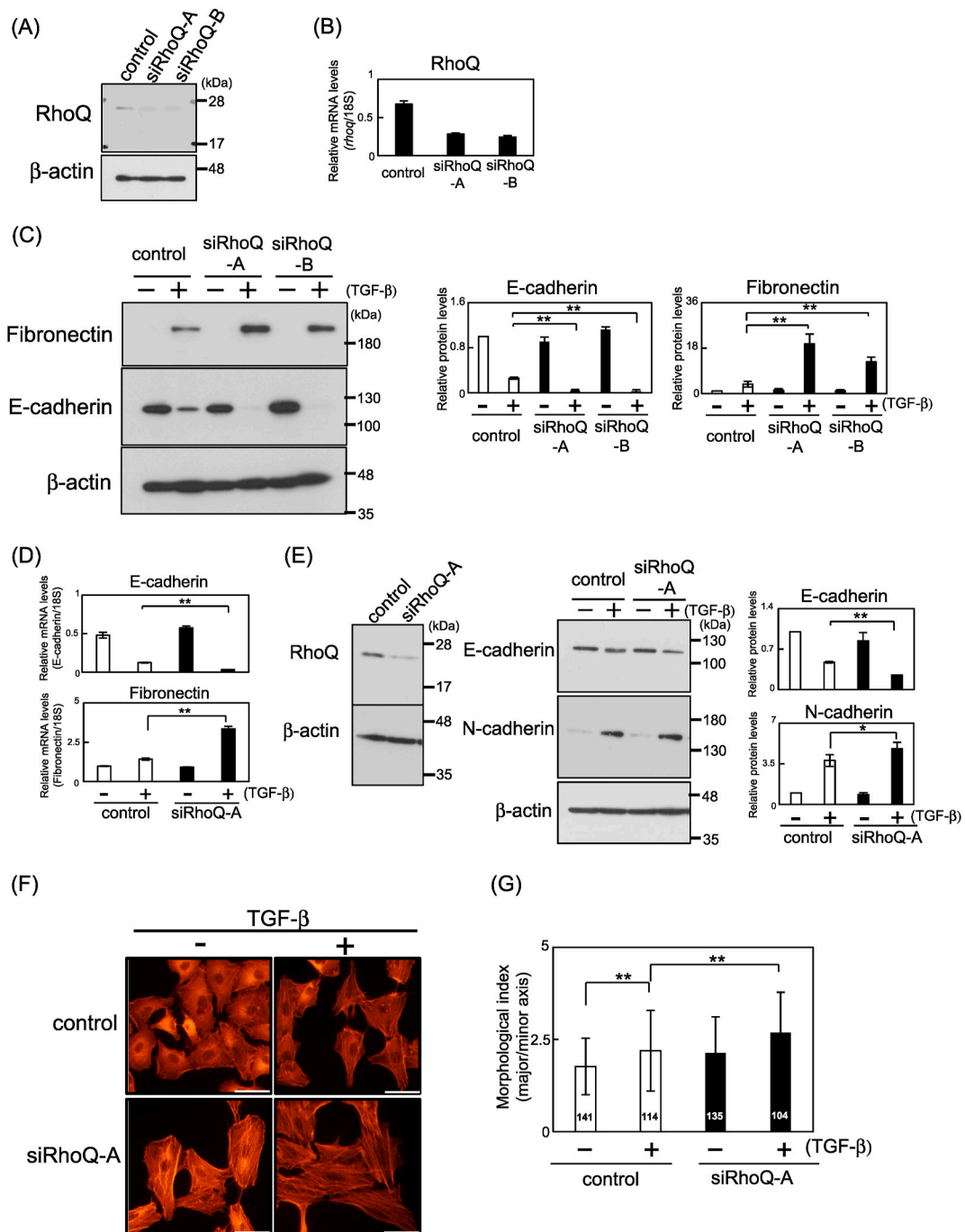
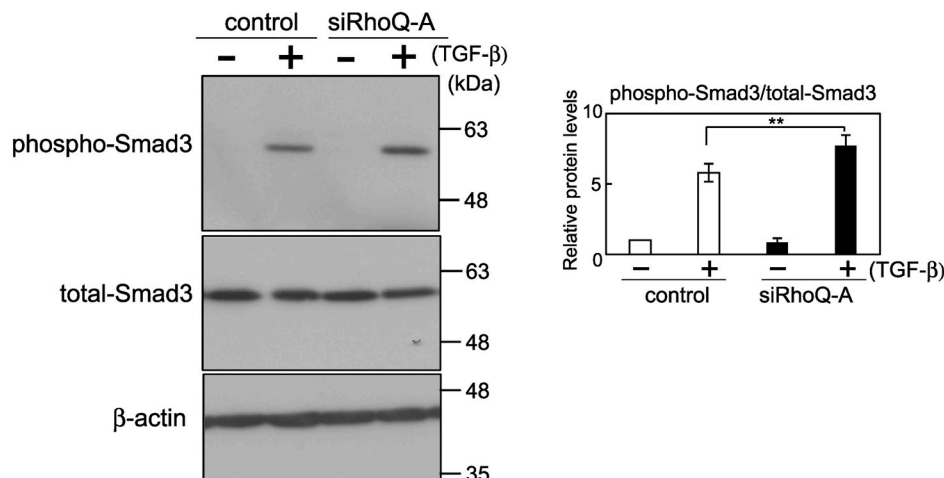


**Fig. 1.** Effect of knockdown of RhoQ on the expression levels of epithelial-to-mesenchymal transition (EMT)-related genes in lung adenocarcinoma cell lines. (A) Cell lysates were prepared from A549 cells transfected with siLuciferase, siRhoQ-A, and siRhoQ-B. Protein levels of RhoQ and  $\beta$ -actin, a loading control, were determined by Western blot analysis. (B) The mRNA levels of RhoQ were assessed by Q-PCR using specific primers for RhoQ. 18S rRNA was used as the internal control for normalization. Each column shows mean  $\pm$  standard deviation (SD) ( $n = 3$ ). (C) Cell lysates from control and RhoQ-knockdown cells treated with 1 ng/mL TGF- $\beta$ 1 for 48 h were analyzed on Western blot probed with antibodies against E-cadherin and fibronectin. Each column shows mean  $\pm$  SD ( $n = 4$ ). (D) The mRNA levels of E-cadherin and fibronectin were assessed by Q-PCR. Expression of E-cadherin and fibronectin mRNA in control and RhoQ-knockdown cells treated with TGF- $\beta$ 1 for 48 h. Each column shows mean  $\pm$  SD ( $n = 3$ ). (E) Cell lysates were prepared from PC-9 cells transfected with siLuciferase and siRhoQ-A. Cell lysates from control and RhoQ-knockdown cells treated with 5 ng/mL TGF- $\beta$ 1 for 48 h were analyzed on Western blot probed with antibodies against E-cadherin and N-cadherin. Each column shows mean  $\pm$  SD ( $n = 3$ ). (F) F-actin in RhoQ-knockdown A549 cells treated with 1 ng/mL TGF- $\beta$ 1 for 48 h is visualized with TRITC-conjugated phalloidin. Bars = 25  $\mu$ m. (G) The ratio of cell major axis and minor axis in A549 cells was measured to evaluate the degree of cell elongation. Each column shows mean  $\pm$  SD; the number of cells used for these experiments is shown in each bar's parentheses. Significant differences are denoted as \*\* $p < 0.01$ , \* $p < 0.05$ .

(A)



(B)

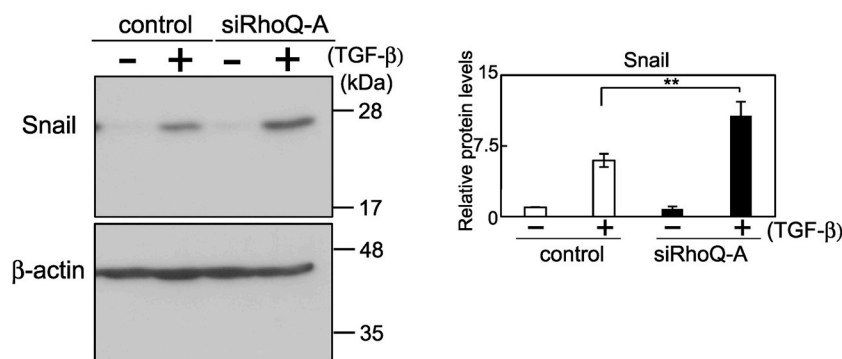


**Fig. 2.** Effect of knockdown of RhoQ on Smad3 phosphorylation and Snail expression during TGF- $\beta$ -mediated EMT in A549 cells. (A) Smad3 phosphorylation and expression of total Smad3 in control and RhoQ-knockdown cells undergoing TGF- $\beta$ -mediated EMT were determined by Western blot analysis. Each column shows mean  $\pm$  SD (n = 4). (B) The expression level of Snail protein in RhoQ-knockdown cells undergoing EMT was determined by Western blot analysis. Each column shows mean  $\pm$  SD (n = 4). Significant differences are denoted as \*\*p < 0.01.

### 2.10. Statistical tests

Statistical analyses were performed using R (<http://cran.r-project.org/>). Statistical significance was determined for multigroup analysis using one-way ANOVA with Tukey–Kramer post-hoc testing.

## 3. Results

### 3.1. Repression of RhoQ expression promotes TGF- $\beta$ 1-mediated EMT in LUAD cells

We performed knockdown experiments to determine the role of RhoQ on EMT in A549 cells. A549 cells were transfected with two different human RhoQ siRNAs (siRhoQ-A and siRhoQ-B) and a control siRNA. Western blot and Q-PCR analysis revealed that the introduction of siRhoQ-A and -B effectively downregulated the expression of endogenous RhoQ (Fig. 1A and B). We examined the effect of RhoQ on the expression levels of EMT-related genes in A549 cells. The protein level of E-cadherin, an epithelial marker, decreased significantly in two RhoQ-knockdown cells treated with TGF- $\beta$ 1 compared to control cells, as shown in Fig. 1C. On the other hand, in RhoQ-knockdown cells, the mesenchymal marker fibronectin protein level increased (Fig. 1C). Furthermore, Q-PCR revealed that fibronectin mRNA expression was increased in RhoQ-knockdown cells. In contrast, E-cadherin expression was decreased in RhoQ-knockdown cells treated with TGF- $\beta$ 1 compared to control cells (Fig. 1D).

We then investigated the effect of RhoQ knockdown on TGF- $\beta$ -induced EMT in PC-9, a LUAD cell line distinct from A549. PC-9, like

A549 cells, has been used for TGF-induced EMT experiments [27]. Furthermore, Ying et al. stated that PC-9 cells show higher metastatic potential than A549 cells [28]. As in the A549 studies, E-cadherin expression was significantly reduced in RhoQ-knockdown cells, whereas the expression of the mesenchymal marker N-cadherin was increased (Fig. 1E).

The role of RhoQ in morphology change during EMT was then investigated. The number of long and thick actin stress fibers increased in RhoQ-knockdown cells treated with TGF- $\beta$ 1 compared to control cells, according to TRITC-conjugated phalloidin staining (Fig. 1F). In addition, we calculated the ratios of the major and minor cell axes and assessed the transition to spindle-shaped morphology. As a result, when RhoQ-knockdown cells were treated with TGF- $\beta$ 1, their cell elongation was significantly greater than in control cells (Fig. 1G). Examination of EMT marker gene expression and cell morphology suggested that repression of RhoQ expression induced TGF- $\beta$ -mediated EMT in LUAD cells.

### 3.2. Reduction of RhoQ expression enhances the phosphorylation level of Smad3 and snail expression at the early stage of EMT in A549 cells

Binding of TGF- $\beta$  to its receptor phosphorylates R-Smads such as Smad3 and increases the expression of Snail, a transcription factor that promotes EMT. Previous research found that Smad3 phosphorylation and Snail expression increased in A549 cells 10 h after TGF- $\beta$ 1 treatment [7]. As a result, we investigated whether RhoQ was involved in regulating Smad3 phosphorylation and Snail expression 10 h after TGF- $\beta$ 1 stimulation. Although the total Smad3 level did not differ between

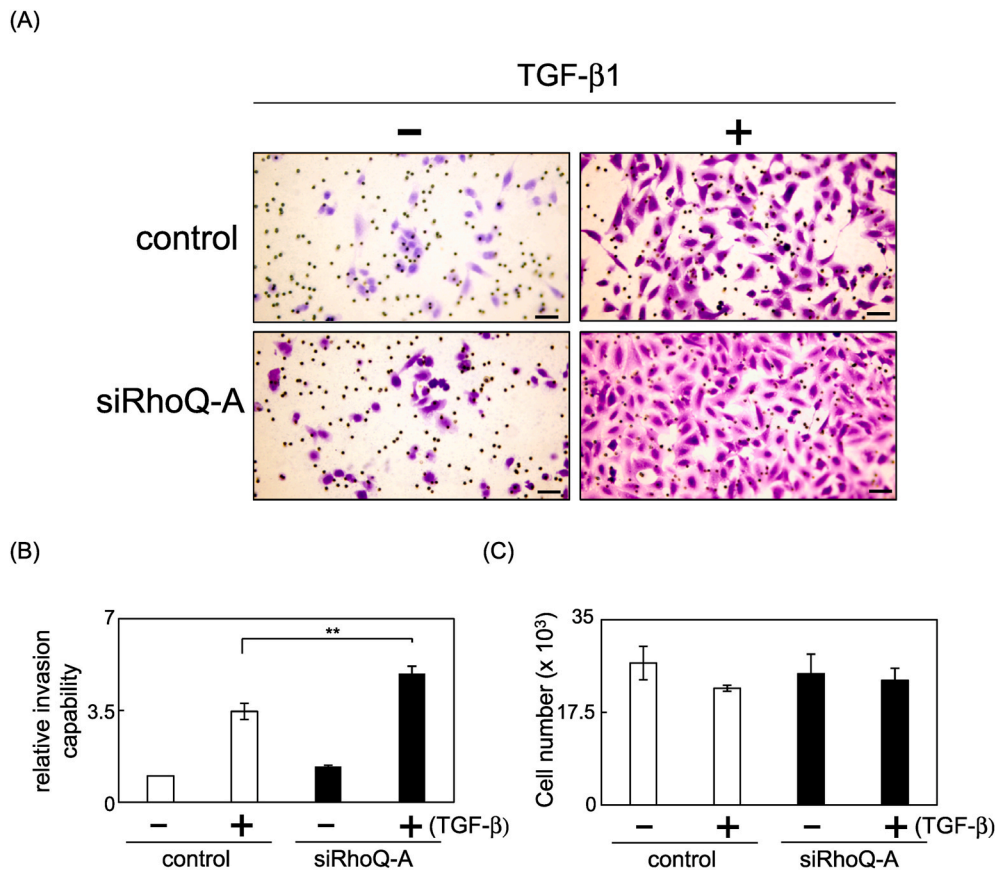


**Fig. 3.** Effect of RhoQ knockdown on the invasion capacity of A549 cells undergoing TGF- $\beta$ -induced EMT. The cells that invaded the underside of the transwell insert were stained and counted. (A) Representative images of invading cells. Bars = 100  $\mu$ m. (B) The mean number of invaded cells in the field was calculated. Data were obtained from three independent experiments. Each column shows mean  $\pm$  SD. (C) Cells undergoing EMT were plated and counted after 24 h to evaluate proliferation capacity. Each column shows mean  $\pm$  SD (n = 4). Significant differences are denoted as \*\* $p$  < 0.01.

RhoQ-knockdown cells and control cells, the phosphorylation level of Smad3 increased significantly in RhoQ-knockdown cells stimulated with TGF- $\beta$ 1 compared to control cells, as shown in Fig. 2A. As with the phosphorylation level of Smad3, the expression level of Snail was also significantly upregulated in RhoQ-knockdown cells treated with TGF- $\beta$ 1 (Fig. 2B). These findings suggested that RhoQ played a role in the regulation of TGF- $\beta$ /Smad signaling during EMT in A549 cells.

### 3.3. Reduction of RhoQ expression upregulates invasion of A549 cells undergoing TGF- $\beta$ -induced EMT

Subsequently, we investigated the effect of RhoQ knockdown on A549 cell invasion after TGF- $\beta$ -induced EMT. RhoQ silencing significantly increased the number of invaded cells in an invasion assay using Matrigel-coated transwell chambers (Fig. 3A and B). However, reduced RhoQ expression did not affect the growth of A549 cells that had undergone EMT (Fig. 3C). These findings suggested that reduced RhoQ expression increased the invasion capacity of A549 cells that had undergone EMT.

### 3.4. RhoQ expression is related to prognosis in LUAD

The Kaplan-Meier plotter, an online database, were used to investigate the relationship between RhoQ expression and prognosis in LUAD and LUSC [26,29]. Our analysis revealed that patients with low RhoQ expression had a significantly worse prognosis ( $p = 2.1e-09$ ) than patients with high RhoQ expression in LUAD. In contrast, there is no correlation between RhoQ expression and prognosis in lung squamous cell carcinoma ( $p = 0.94$ ), the other type of NSCLC (Fig. 4A). These findings suggested that low RhoQ levels were associated with poor overall survival in patients with LUAD.

## 4. Discussion

In the present study, we demonstrated that reduction of RhoQ expression promoted TGF- $\beta$ -mediated EMT and increased the invasion ability in A549 cells. Furthermore, repression of RhoQ expression enhanced cell elongation, smad3 phosphorylation levels, and invasive potential during the EMT process of PC-9 cells, a more malignant LUAD than A549 (Supplementary Figs. S1–S3). In addition, Kaplan-Meier plotter analysis showed that low RhoQ levels were linked with poor overall survival in patients with LUAD. Overall, RhoQ functions as a negative regulator of EMT through the regulation of TGF- $\beta$  signaling (Fig. 4B), and its decreased expression may contribute to the increased malignant potential of LUAD.

As shown in Fig. 2, reduction of RhoQ expression increases the phosphorylation level of Smad3 during the EMT process, implying that RhoQ may have a function of suppressing the TGF/Smad signaling during EMT in LUAD cells. Although the relationship between RhoQ and TGF- $\beta$  signaling is uncertain, some Rho family proteins have been shown to inhibit TGF- $\beta$  signaling. Yamamoto et al. discovered that Rac inhibits p38 MAP kinase in osteoblasts, which inhibits TGF- $\beta$ -stimulated vascular endothelial growth factor synthesis [30]. Furthermore, Rac1b, an alternatively spliced Rac1 isoform, suppressed TGF- $\beta$ 1-induced phosphorylation of Smad3 in pancreatic ductal adenocarcinoma Panc-1 cells through repression of the mitogen-activated protein kinase-extracellular signal-related kinase (MEK-ERK) signaling pathway [31]. It is necessary to evaluate the roles of RhoQ on intracellular signaling pathways, including p38 MAPK and MEK signaling to clarify how RhoQ regulates TGF- $\beta$ -Smad signaling.

We recently demonstrated that RhoJ knockdown accelerated TGF- $\beta$ -mediated EMT in A549 cells via regulation of Smad3 phosphorylation [7]. Despite their high similarity, the two proteins, RhoQ and RhoJ, may serve different physiological functions. RhoJ, for example, is highly

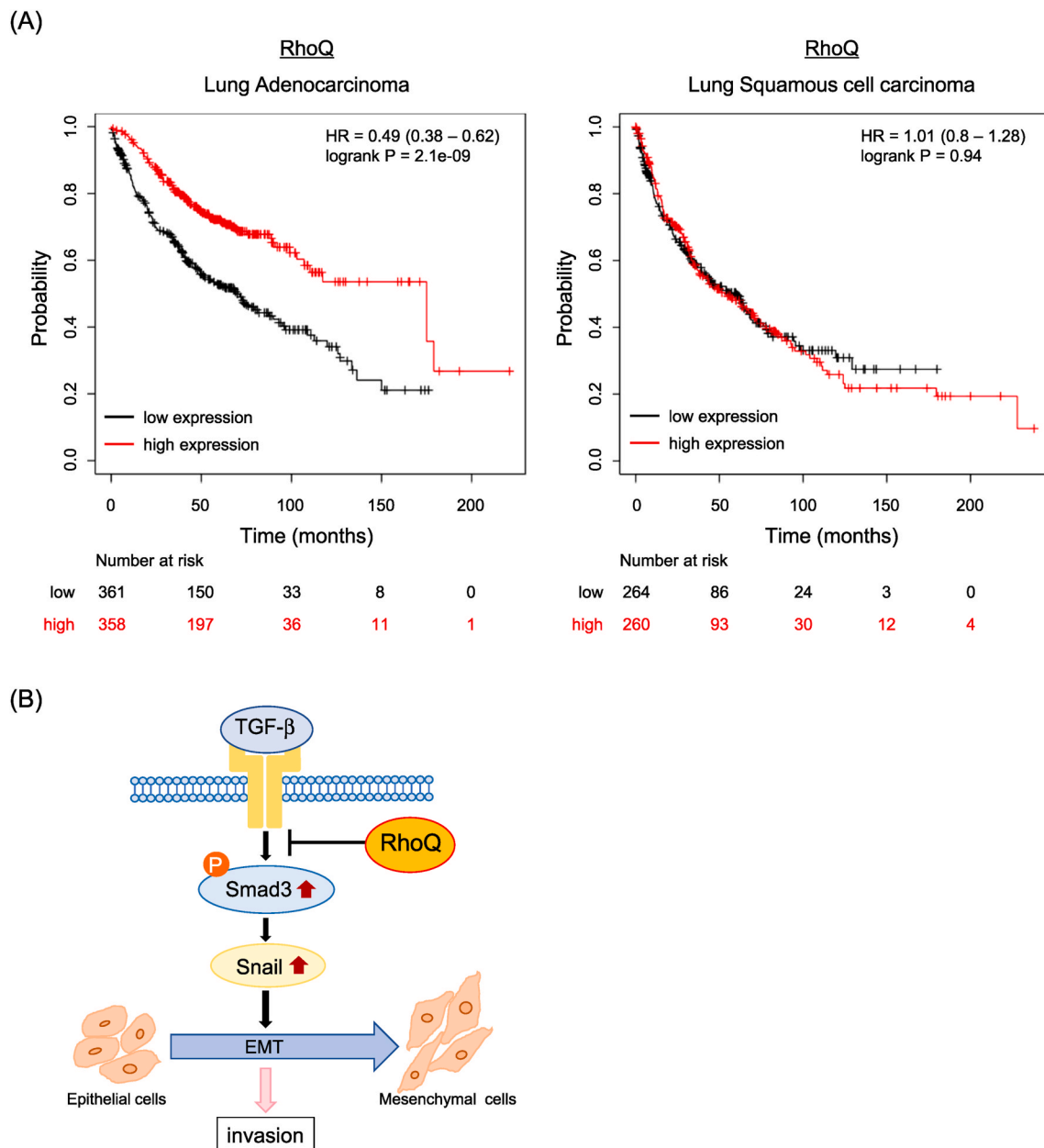


**Fig. 4.** Kaplan–Meier analysis in patients with lung adenocarcinoma with high or low expression of RhoQ. Prognosis of patients with lung cancer expression of RhoQ. Correlation between RhoQ expression and prognosis in lung cancers using the online Kaplan–Meier plotter. LUAD is 719 patients (low:361, high:358) and LUSC is 524 patients (low:264, high:260), respectively.

expressed in endothelial cells and is required for angiogenesis [32]. RhoQ, on the other hand, stimulates neurite outgrowth in PC12, N1E-115, and cultured dorsal root ganglia cells [33]. Furthermore, Vignal et al. found that RhoJ-overexpressing cells have a limited number of ruffle-like protrusions on their dorsal membrane, which are associated with large intracytoplasmic vesicles, whereas RhoQ overexpression results in several filopodial extensions in rat embryo fibroblasts [34]. Although RhoQ plays a critical role in insulin-stimulated GLUT4 translocation and glucose uptake in mature adipocytes [16], RhoJ is not involved in glucose uptake and promotes adipocyte differentiation at the early stages of adipocyte differentiation [35]. In light of these findings, both RhoQ and RhoJ suppressed EMT in LUAD, but their regulatory mechanisms may be distinct. Since the effector proteins contribute significantly to the function of Rho GTPase, it is necessary to clarify which effector proteins RhoQ and RhoJ interact with in the EMT process of LUAD.

Based on the knockdown experiments and Kaplan–Meier plotter analysis, decreased RhoQ expression may contribute to the progression of LUAD. Anusewicz et al. described that LUAD generally grows more slowly with smaller masses than LUSC of the same stage, but LUAD tends to initiate metastasis at the early stage [36]. Furthermore, Krause et al. reported that distant metastases are more common in LUAD than in LUSC [37]. These findings suggested that the relationship between reduced RhoQ expression and poor prognosis may be observed in highly metastatic cancer cells. It is also possible that decreased RhoQ expression may contribute to the higher metastatic potential in LUAD compared to LUSC. It has also been reported that the LUSC cell lines, NCI-H460 and NCI-H520 are induced to EMT by TGF- $\beta$  [38]. It is necessary to examine whether RhoQ affects TGF- $\beta$ -mediated EMT in the LUSC cell lines. Furthermore, the discovery and analysis of promoter regions that regulate RhoQ expression may lead to the development of RhoQ-targeting drugs.

In conclusion, we discovered for the first time that suppression of RhoQ expression promotes TGF- $\beta$ -mediated EMT in LUAD cells and contributes to poor prognosis in patients with LUAD. Further research, including identifying RhoQ promoter regions and effector proteins, will aid in elucidating the role of RhoQ in LUAD metastasis.

### Funding

This study was partly supported by grants from the Japan Society for the Promotion of Science (JSPS) and by the Suzuken Memorial Foundation.

### Author contributions

M.N. conceived and designed the experiments. K.S. and M.N. performed the experiments. K.S., S.S., and M.N. analyzed the data. S.S. and M.N. wrote the paper.

### Declaration of competing interest

There are no conflicts of interest to declare.

### Appendix A. Supplementary data

Supplementary data to this article can be found online at <https://doi.org/10.1016/j.bbrep.2022.101346>.

### References

- [1] S. Saab, H. Zalzal, Z. Rahal, et al., Insights into lung cancer immune-based biology, prevention, and treatment, *Front. Immunol.* 11 (2020) 159.
- [2] L. Junyuan, Z. Yuting, T. Jie, et al., Heat shock factor 2-binding protein promotes tumor progression via activation of MAPK signaling pathway in lung adenocarcinoma, *Bioengineered* 13 (2022) 10324–10334.
- [3] S.T. Kundu, B.L. Rodriguez, L.A. Gibson, et al., The microRNA-183/96/182 cluster inhibits lung cancer progression and metastasis by inducing an interleukin-2-mediated antitumor CD8<sup>+</sup> cytotoxic T-cell response, *Genes Dev.* 36 (2022) 582–600.
- [4] V. Ramesh, T. Brabletz, P. Ceppi, EMT in cancer with repurposed metabolic inhibitors, *Trends in Cancer* 6 (2020) 942–950.
- [5] Y. Tsubakihara, A. Moustakas, Epithelial-mesenchymal transition and metastasis under the control of transforming growth factor  $\beta$ , *Int. J. Mol. Sci.* 19 (2018) 3672.
- [6] G. Cantelli, E. Crosas-Molist, M. Georgouli, et al., TGF $\beta$ -induced transcription in cancer, *Semin. Cancer Biol.* 42 (2017) 60–69.
- [7] M. Nozaki, M. Nishizuka, Repression of RhoJ expression promotes TGF- $\beta$ -mediated EMT in human non-small-cell lung cancer A549 cells, *Biochem. Biophys. Res. Commun.* 566 (2021) 94–100.
- [8] T. Zeng, C. Chen, P. Yang, et al., A protective role for RHOJ in non-small cell lung cancer based on integrated bioinformatics analysis, *J. Comput. Biol.* 27 (2020) 1092–1103.
- [9] R.B. Haga, A.J. Ridley, Rho GTPases: regulation and roles in cancer cell biology, *Small GTPases* 7 (2016) 207–221.
- [10] N.S. Clayton, A.J. Ridley, Targeting Rho GTPase signaling networks in cancer, *Front. Cell Dev. Biol.* 8 (2020) 222.
- [11] L. Zhang, M. Gallup, L. Zlock, et al., Rac1 and Cdc42 differentially modulate cigarette smoke-induced airway cell migration through p120-catenin-dependent and -independent pathways, *Am. J. Pathol.* 182 (2013) 1986–1995.
- [12] Y. Dong, X. Jin, Z. Sun, et al., MiR-186 inhibited migration of NSCLC via targeting cdc42 and effecting EMT process, *Mol. Cell* 40 (2017) 195–201.
- [13] G.A. Murphy, P.A. Solski, S.A. Jillian, et al., Cellular functions of TC10, a Rho family GTPase: regulation of morphology, signal transduction and cell growth, *Oncogene* 18 (1999) 3831–3845.
- [14] A. Fujita, S. Koinuma, S. Yasuda, GTP hydrolysis of TC10 promotes neurite outgrowth through exocytic fusion of Rab11- and L1-containing vesicles by releasing exocyst component Exo70, *PLoS One* 8 (2013), e79689.
- [15] S. Dupraz, D. Grassi, M.E. Bernis, et al., The TC10-Exo70 complex is essential for membrane expansion and axonal specification in developing neurons, *J. Neurosci.* 29 (2009) 13292–13301.
- [16] S.H. Chiang, C.A. Baumann, M. Kanzaki, et al., Insulin-stimulated GLUT4 translocation requires the CAP-dependent activation of TC10, *Nature* 410 (2001) 944–948.
- [17] M. Hülsemann, C. Sanchez, P.V. Verkhusa, et al., TC10 regulates breast cancer invasion and metastasis by controlling membrane type-1 matrix metalloproteinase at invadopodia, *Commun. Biol.* 4 (2021) 1091.
- [18] S.W. Han, H.P. Kim, J.Y. Shin, et al., RNA editing in RHOQ promotes invasion potential in colorectal cancer, *J. Exp. Med.* 211 (2014) 613–621.
- [19] X.F. Chen, H.J. Zhang, H.B. Wang, et al., Transforming growth factor- $\beta$ 1 induces epithelial-to-mesenchymal transition in human lung cancer cells via PI3K/Akt and MEK/Erk1/2 signaling pathways, *Mol. Biol. Rep.* 39 (2012) 3549–3556.
- [20] G.M. Krentz, J.P. Collard, K. Thompson, et al., A microRNA signature of response to erlotinib is descriptive of TGF $\beta$  behaviour in NSCLC, *Sci. Rep.* 7 (2017) 4202.
- [21] A.C.M. Sousa-Squiavinato, M.R. Rocha, P. Barcellos-de-Souza, et al., Cofilin-1 signaling mediates epithelial-mesenchymal transition by promoting actin cytoskeleton reorganization and cell-cell adhesion regulation in colorectal cancer cells, *Biochim. Biophys. Acta Mol. Cell Res.* 1866 (2019) 418–429.
- [22] M. Nishizuka, R. Komada, M. Imagawa, Knockdown of RhoE expression enhances TGF- $\beta$ -induced EMT (epithelial-to-mesenchymal transition) in cervical cancer HeLa cells, *Int. J. Mol. Sci.* 20 (2019) 4697.
- [23] Y. Arima, Y. Inoue, T. Shibata, et al., Rb depletion results in deregulation of E-cadherin and induction of cellular phenotypic changes that are characteristic of the epithelial-to-mesenchymal transition, *Cancer Res.* 68 (2008) 5104–5112.
- [24] A. Morén, E. Raja, C.H. Heldin, et al., Negative regulation of TGF $\beta$  signaling by the kinase LKB1 and the scaffolding protein LIP1, *J. Biol. Chem.* 286 (2011) 341–353.
- [25] M. Goto, S. Osada, M. Imagawa, et al., FAD104, a regulator of adipogenesis, is a novel suppressor of TGF- $\beta$ -mediated EMT in cervical cancer cells, *Sci. Rep.* 7 (2017), 16365.
- [26] A. Lanczky, B. Györfy, Web-based survival analysis tool tailored for medical research (KMplot): development and implementation, *J. Med. Internet Res.* 23 (2021), e27633.
- [27] J. Zhang, Y.L. Chen, G. Ji, et al., Sorafenib inhibits epithelial-mesenchymal transition through an epigenetic-based mechanism in human lung epithelial cells, *PLoS One* 8 (2013), e6495435.
- [28] Z. Ying, H. Tian, Y. Li, et al., CCT6A suppresses SMAD2 and promotes prometastatic TGF- $\beta$  signaling, *J. Clin. Invest.* 127 (2017) 1725–1740.
- [29] B. Györfy, P. Surowiak, J. Budczies, et al., Online survival analysis software to assess the prognostic value of biomarkers using transcriptomic data in non-small-cell lung cancer, *PLoS One* 8 (2013), e82241.
- [30] N. Yamamoto, T. Otsuka, A. Kondo, et al., Rac limits TGF- $\beta$ -induced VEGF synthesis in osteoblasts, *Mol. Cell. Endocrinol.* 405 (2015) 35–41.
- [31] R. Zinn, H. Otterbein, H. Lehnert, et al., RAC1B: a guardian of the epithelial phenotype and protector against epithelial-mesenchymal transition, *Cells* 8 (2019) 1569.
- [32] T.T. Shi, G. Li, H.T. Xiao, The role of RhoJ in endothelial cell biology and tumor pathology, *BioMed Res. Int.* 2016 (2016), 6386412.
- [33] N.G. Gracias, N.J. Shirkey-Son, U. Hengst, Local translation of TC10 is required for membrane expansion during axon outgrowth, *Nat. Commun.* 25 (2014) 3506.
- [34] E. Vignal, M. Toledo, F. Comunale, et al., Characterization of TCL, a new GTPase of the rho family related to TC10 and Cdc42, *J. Biol. Chem.* 275 (2000) 36457–36464.
- [35] M. Nishizuka, E. Arimoto, T. Tsuchiya, et al., Crucial role of TCL/TC10beta L, a subfamily of Rho GTPase, in adipocyte differentiation, *J. Biol. Chem.* 278 (2003) 15279–15284.
- [36] D. Anusewicz, M. Orzechowska, A.K. Bednarek, Lung squamous cell carcinoma and lung adenocarcinoma differential gene expression regulation through pathways of Notch, Hedgehog, Wnt, and ErbB signalling, *Sci. Rep.* 10 (2020), 21128.
- [37] A. Krause, L. Roma, T. Lorber, et al., Genomic evolutionary trajectory of metastatic squamous cell carcinoma of the lung, *Transl. Lung Cancer Res.* 4 (2021) 1792–1803.
- [38] W.C. Chiou, C. Huang, Z.J. Lin, et al., A-viniferin and e-viniferin inhibited TGF- $\beta$ 1-induced epithelial-mesenchymal transition, migration and invasion in lung cancer cells through downregulation of vimentin expression, *Nutrients* 14 (2022):2294.